The surface-atmosphere exchange of carbon dioxide, water, and sensible heat across a dryland wheat-fallow rotation

Authors: Elizabeth S.K. Vick, Paul C. Stoy, Angela C.I. Tang, and Tobias Gerken

Vick, Elizabeth S. K., Paul C. Stoy, Angela C. I. Tang, and Tobias Gerken. "The surface-atmosphere exchange of carbon dioxide, water, and sensible heat across a dryland wheat-fallow rotation." Agriculture, Ecosystems & Environment 223 (September 16, 2016): 129-140. DOI: 10.1016/j.agee.2016.07.018.

The surface-atmosphere exchange of carbon dioxide, water, and sensible heat across a dryland wheat-fallow rotation

Elizabeth S.K. Vick[a], Paul C. Stoy[a,*], Angela C.I. Tang[a], Tobias Gerken[a,b]

[a] Department of Land Resources and Environmental Sciences, Montana State University, Bozeman, MT 59717, USA
[b] Department of Meteorology, The Pennsylvania State University, University Park, PA 16802, USA

ABSTRACT

Summer fallow – the practice of keeping a field out of production during the growing season – is a common practice in dryland wheat (*Triticum aestivum* L.) cropping systems to conserve soil water resources. Fallow also depletes soil carbon stocks and thereby soil quality. The area of summer fallow has decreased by tens of millions of hectares since the 1970s in the northern North American Great Plains as producers have recognized that avoiding fallow usually confers both economic and soil conservation benefits. Observed summertime cooling across parts of this region has coincided with fallow reduction, suggesting that the role of fallow in atmospheric processes needs to be ascertained. We measured carbon dioxide, latent heat, and sensible heat flux across a winter wheat – spring wheat – fallow sequence in Montana, USA to determine the effects of dryland crop management on ecosystem carbon resources and energy partitioning at the surface-atmosphere interface. Winter wheat and spring wheat fields were carbon sinks ($F_c = -203 \pm 52$ g C—CO_2 m^{-2} and -107 ± 29 g C—CO_2 m^{-2}), respectively, during the April to September study period, but the fallow field was a carbon source of 135 ± 73 g C—CO_2 m^{-2}. Evapotranspiration in the wheat crops was over 100 mm greater than the 275 ± 39 mm observed in the fallow field during the study period. Modeled maximum daily atmospheric boundary layer height was on average 210 m higher and up to 900 m higher in fallow compared to the spring wheat field with more crossings of the modeled atmospheric boundary layer and lifted condensation level, suggesting that regional studies of the effects of fallow on near-surface temperature and moisture are necessary to understand the effects of fallow reduction on regional climate dynamics. Results demonstrate that fallow has a detrimental impact to soil carbon resources yet is less water intensive, with consequences for regional climate via its impacts on atmospheric boundary layer development and global climate via its carbon metabolism.

1. Introduction

Wheat (*Triticum aestivum* L.) provides more than 20% of the calories and protein for the global population (Hawkesford et al., 2013) and nearly 220 Mha of wheat was harvested globally in 2013 (FAO, 2013). Wheat therefore plays a central role in not only global food production, but also in the global exchange of water, energy, and climate-relevant trace gases like carbon dioxide between the land surface and the atmosphere (West and Marland, 2002; Buyanovsky and Wagner, 1998).

Our understanding of the interaction between wheat cropping systems and the atmosphere remains incomplete. Wheat has a very low canopy resistance to water vapor transport during its main growth period (Bonan, 2008), and models tend to accurately simulate latent heat flux (*LE*, see Table 1 for a list of abbreviations), and sensible heat flux (*H*) during these periods (Ingwersen et al., 2011). Aspects of the seasonal timing of crop development including ripening (Ingwersen et al., 2011) and management decisions like harvesting (Sus et al., 2010) on surface-atmosphere fluxes continue to challenge ecosystem models. Management practices including crop rotations have been identified as important contributors to carbon metabolism at the field scale (Béziat et al., 2009; Schmidt et al., 2012), but have largely been studied in winter wheat crops and/or mesic cropping systems to date (e.g. Billesbach et al., 2014; Moureaux et al., 2008). Surface-atmosphere exchange in rotations common to dryland cropping systems including spring wheat and chemical fallow (hereafter 'fallow') have been studied less-frequently to date.

Table 1
A list of abbreviations with their definitions.

Abbreviation	Definition
α	Initial slope of the light response curve
α_{PT}	Priestley-Taylor coefficient
β	Gross ecosystem productivity at light saturation
γ	Psychrometric constant
γ^*	Virtual temperature inversion strength
Δh	Change in height of the atmospheric boundary layer
ε_{PT}	Intercept term of the Priestley-Taylor-type model
λ	Latent heat of vaporization
ρ_a	Density of air
ABL	Atmospheric boundary layer
c_p	Specific heat capacity
E_0	Activation energy
ET	Evapotranspiration
F_c	Carbon dioxide flux
G	Soil heat flux
GEP	Gross ecosystem productivity
h	Height of the atmospheric boundary layer
h_{LCL}	Height of the lifting condensation level
H	Sensible heat flux
H_v	Virtual heat flux
LE	Latent heat flux
P	Atmospheric surface pressure
r	Water vapor mixing ratio
RE	Ecosystem respiration
R_n	Net radiation
R_{10}	Ecosystem respiration at an air temperature of 10 °C
s	Slope of the vapor pressure-temperature relationship at saturation
SW_{in}	Incident shortwave radiation
T_a	Air temperature
T_{10}	Air temperature of 10 °C
T_{LCL}	Air temperature at the lifting condensation level
T_t	Reference temperature (227.13 K)
u^*	Friction velocity

Fallow is a common management practice in the dryland wheat-growing regions of the northern North American Great Plains to conserve water for subsequent crops (Lubowski et al., 2006). Fallow however also increases erosion (Wischmeier, 1959) and soil carbon loss (Cihacek and Ulmer, 1995), and fallow-small grain management strategies are not considered sustainable from the soil conservation perspective (Merrill et al., 1999). Management practices are changing. The area of fallow in the Prairie Provinces of Canada has decreased from over 15 Mha in the 1970s to under 2 Mha at the present (Fig. 1) as producers have realized

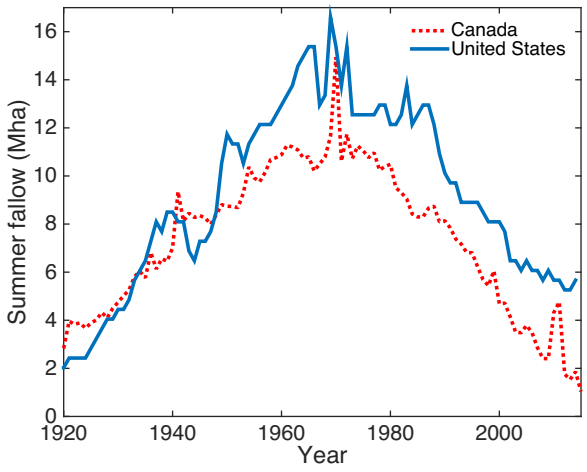

Fig. 1. Trends in summer fallow area from 1920 until the present in Canada (red dashed line) and the United States (blue solid line) using data from Statistics Canada and the United States Department of Agriculture Economic Research Service. (For interpretation of the references to colour in this figure legend, the reader is referred to the web version of this article.)

that the water-savings benefit of fallow is outweighed by the economic losses of not planting (Dhuyvetter et al., 1996). The area under fallow in the United States has likewise decreased from 16 Mha to 6 Mha across the same time frame (Lubowski et al., 2006), largely in the northern Great Plains and other areas of the semiarid West (Fig. 1). Despite the decreasing trend in fallow area across the North American northern Great Plains, fallow remains common in many regions including major land resource area (MLRA) 52 in north-central Montana – the largest wheat-growing region in the state – where some 40% of agricultural lands may remain in fallow in any given year. In contrast, fallow has been reduced in northeastern Montana (MLRA 53) by hundreds of kha over the past decade (Long et al., 2014, 2013) as producers have adopted continuous cropping or alternate cropping practices (Burgess et al., 2012; Miller et al., 2003, 2002).

The widespread decline of fallow in agricultural areas of the Canadian Prairie Provinces (Fig. 1) has coincided with a summertime cooling trend since the 1970s (Betts et al., 2013a, 2013b; Gameda et al., 2007; Mahmood et al., 2014). Extreme temperature events now occur less frequently than in the recent past, maximum summer temperatures have decreased by *ca.* 2 °C, relative humidity has increased by some 7% (Betts et al., 2013b), and summer precipitation has increased by an average of 10 mm/decade across parts of the Canadian Prairie Provinces (Gameda et al., 2007). A remarkable 6 W m^{-2} summer cooling has been observed (Betts et al., 2013a); for reference, anthropogenic greenhouse gasses are responsible for a *ca.* 2.5 W m^{-2} warming globally since the dawn of the Industrial Era (IPCC, 2007). These climate benefits have only occurred during the growing season; fall, winter, and early spring temperatures have followed global trends (Betts et al., 2013b).

Studies suggest that these climate changes are the result of land management, specifically the trend away from leaving fields fallow

during summer (Betts et al., 2013a; Gameda et al., 2007; Mahmood et al., 2014). These large-scale declines in fallow area have resulted in less sensible heat and more water vapor entering the atmosphere and a moister, shallower atmospheric boundary layer (*ABL*) and lower lifted condensation level (*LCL*) with an increased probability of convective precipitation (Betts et al., 2013b; Gameda et al., 2007). In other words, the observed regional climate cooling is broadly consistent with the effects of fallow avoidance on climate processes.

Using a conceptual model, Gameda et al. (2007) suggested that fallow supports an *ABL* height (h) on the order of 2–3 km, but that h is only some 0.5 km over crops. These estimates have not been supported by observations or models, in part because the impacts of field-scale management changes on H and LE, which help determine h, have not been studied to date in wheat-fallow rotations. Doing so is an important step in understanding the role of human management on climate processes in the North American Northern Great Plains.

Cropping systems that include wheat also influence land surface biogeochemistry. Many studies to date have used the eddy covariance technique to find that wheat tends to be a strong carbon sink at the field scale during the growing season, but is infrequently a net annual carbon sink. For example, Anthoni et al. (2004a,b) found that a central European winter wheat field was a sink for atmospheric carbon dioxide during the growing season, but a source of carbon annually, with a net biome productivity of 45–105 g C m^{-2} y^{-1}, indicating a loss of C to the atmosphere when the end products of the wheat crop were accounted for. Crop rotations are also important for carbon metabolism. Béziat et al. (2009) measured the carbon balance of a three-crop rotation and found that the net biome productivity was -161 ± 66 g C m^{-2} y^{-1} in winter wheat, but a maize crop at the same site a year earlier was a carbon source of 372 ± 78 g C m^{-2} y^{-1} due in part to residue from previous crops. These observations emphasize the importance of studying crop rotations for a comprehensive understanding of the impacts of agriculture on surface-atmosphere exchange.

Here, we use the eddy covariance technique to measure the surface-atmosphere exchange of carbon dioxide (F_c), LE, and H across a dryland winter wheat – spring wheat – fallow sequence in central Montana, USA. We quantify differences in surface fluxes during the April–September growing period and use models of h and the height of the lifted condensation level (h_{LCL}) driven by observed surface-atmosphere energy flux and near-surface air temperature and humidity to help us understand the physical mechanisms that underlie the observed effects of agricultural management on *ABL*, *LCL*, and regional climate processes (Gameda et al., 2007). We additionally discuss the impacts of wheat and fallow on carbon and water resources to provide information to producers for land management decisions.

2. Materials and methods

2.1. Site description

Eddy covariance and micrometeorological measurements were made in two fields in central Montana, USA. Measurements were made on the first field during 2013 when it was planted with winter wheat, and during 2014 when it was planted with spring

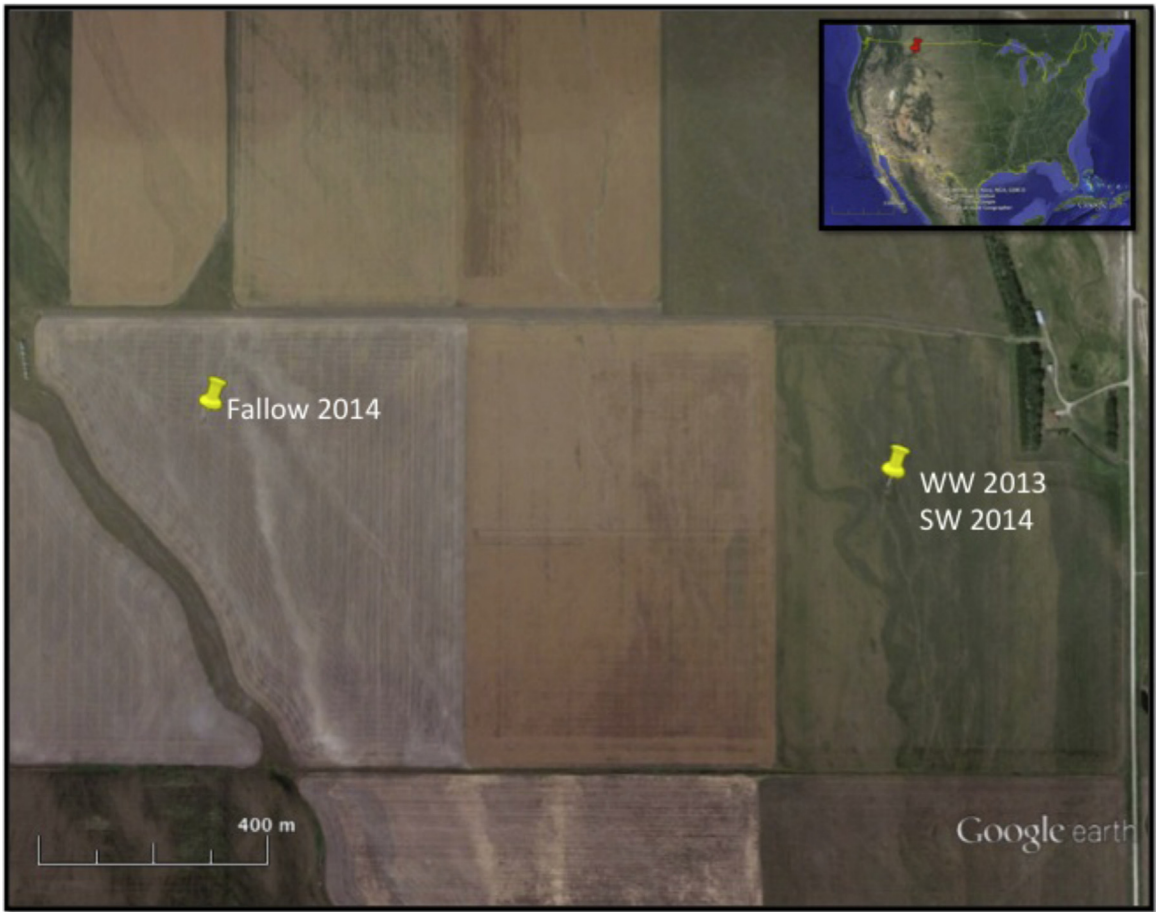

Fig. 2. A map of the winter wheat (WW 2013) and spring wheat (SW 2014) tower location and the fallow (2014) tower location in central Montana, USA. (Image date: 7/25/2014, Google Earth).

wheat. Measurements in the second field were made during 2014 when it was held in fallow.

The first field was planted with winter wheat in autumn, 2012 following a year of chemical fallow. In March 2013, a 3 m tower with eddy covariance and micrometeorological instrumentation was installed in this field at 46° 59′ 41.1″ N, 109° 36′ 49.5″ W (Fig. 2). Eddy covariance instrumentation was mounted at 1.8 m with a fetch of 200 m from the nearest field edge to the west. The winter wheat crop was harvested on August 7, 2013 and instruments were left on the tower until September 2013, when they were removed for calibration and reinstalled. The tower was moved to accommodate the planting of spring wheat on May 5, 2014 and it measured spring wheat during the 2014 growing season. It was removed in September 2014 following the spring wheat harvest on August 18, 2014.

A second tower of identical height and instrumentation height was installed during spring, 2014, at 46° 59′ 44.8″ N, 109° 37′ 46.3″ W in a no-till chemical fallow field that was planted with spring wheat the previous year. Chemical treatments were applied to discourage weedy growth during the study period, with the exception of the immediate vicinity of the tower to avoid damaging sensors. The fallow field was two fields to the west of the first (wheat) field, and the fallow field tower was 1.2 km from the wheat field tower (Fig. 2). The minimum fetch was 200 m to the southwest. For the purposes of this study, measurements from all fields are studied for the April-September period – hereafter the 'study period' – that encompasses the main growing season.

Mean annual temperature and precipitation were 6.6 °C and 388 mm, respectively, in Moccasin, MT where the Montana State University Central Agricultural Research Center is located some 25 km from the study fields. The slope of both fields was less than 0.5° on Judith and Danvers clay loams.

2.2. Measurements

2.2.1. Meteorological measurements

Micrometeorological variables were measured at both towers as summarized in Table 2. Canopy heights and snow depths were measured using a SR50A-L sonic depth sensor (Campbell Scientific Inc., Logan, UT, USA) at the wheat tower. Incident shortwave (SW_{in}), outgoing shortwave, incident longwave, outgoing longwave radiation, and thereby net radiation (R_n) were measured at both towers using NR01 four-component net radiometers (Hukseflux, Delft, The Netherlands) mounted at 1.8 m above the soil surface. Air temperature (T_a) and relative humidity were measured using HMP45C temperature and relative humidity probes (Vaisala, Vantaa, Finland) at 2 m. Soil heat flux (G) was measured using self-calibrating HFP01 heat flux plates (Hukseflux) at 5 cm below the soil surface. Soil moisture was measured at 5 cm and 10 cm using two CS616 time domain reflectometer sensors (Campbell Scientific) in the wheat field and two CS650 sensors (Campbell Scientific) in the fallow field. Soil temperature was measured at multiple depths using copper-constantan thermocouples in the wheat field and the CS650 sensors in the fallow field. Measurements were made every minute and half-hour averages were stored using CR3000 and CR1000 data loggers (Campbell Scientific).

Table 2
Variables measured at each site (see Table 1) along with sensor type. W: Wheat (winter wheat in 2013, spring wheat in 2014), F: Fallow (2014).

Measurement	Sensor(s)	Site
SW_{in}	NR01 net radiometer	W, F
R_n	NR01 net radiometer	W, F
Canopy height	SR50 sonic distance sensor	W
T_a and relative humidity	HMP-50 temperature/relative humidity probe	W, F
G	HFP01 heat flux plate	W, F
H	CSAT-3	W, F
LE	CSAT-3 and LI-7200	W, F
F_c	CSAT-3 and LI-7200	W, F

2.2.2. Turbulent flux measurements

F_c and LE were measured using the eddy covariance technique. This involved the coupling of CSAT-3 sonic anemometers (Campbell Scientific) with LI-7200 CO_2/H_2O enclosed infrared gas analyzers (LiCor, Lincoln, NE) installed 1.8 m above the ground surface on both towers. H was measured using the CSAT-3 sonic anemometers. Data were recorded at 10 Hz on CR3000 data loggers (Campbell Scientific) and processed into half-hourly flux sums using EddyPro (LiCor). Eddy covariance processing steps involved double rotation rather than the planar fit method given the rapid changes in wheat canopy height (Kaimal and Finnegan, 1994), covariance maximization for time lag detection (Mauder and Foken, 2004), and plausibility ranges of five standard deviations from the mean for vertical velocity and 3.5 standard deviations from the mean for CO_2 and H_2O concentrations. Negative values refer to fluxes from the atmosphere to the surface following the micrometeorological convention.

Surface-atmosphere fluxes are often underestimated by eddy covariance measurements, especially during periods of insufficient turbulent exchange that usually occur at night (Aubinet et al., 2000; Falge et al., 2001a; Gu et al., 2005; Papale et al., 2006; Reichstein et al., 2005). A friction velocity (u^*) filter following Reichstein et al. (2005) was applied to the data set to identify and filter periods of insufficient turbulence. F_c measurements made during night, defined as periods for which the solar zenith angle exceeded 90°, were binned into six T_a classes for three month periods and further binned into twenty u^* classes. The u^* filter was chosen to be the value at which the mean value of the F_c observations in a given u^* class first exceeded 95% of the remaining F_c observations at higher values of u^*. u^* threshold values determined using this approach exhibited trivial differences (not shown) from a statistical approach in which the u^* threshold was determined as the u^* class at which the F_c observations were not statistically different than F_c observations at higher u^* as determined by a one-sided t-test following Papale (2012). Nighttime F_c observations that occurred under insufficient u^*, and F_c observations that exceeded logical upper bounds of 20 $\mu mol\, m^{-2}\, s^{-1}$ and lower bounds of -35 $\mu mol\, m^{-2}\, s^{-1}$ determined using probability distribution functions were excluded from the data record.

2.3. Gapfilling and data processing

Missing data occurred due to power outages and equipment malfunction, as well as damage to wires by animals. Missing SW_{in}, T_a, relative humidity, and soil temperature data were gapfilled using linear regression from the neighboring tower if data were available. If data from the neighboring tower were also missing, data from the Moccasin Soil Climate Analysis Network (SCAN) site, located 25 km from the study fields, were used in the gapfilling procedure.

2.3.1. Gapfilling soil heat flux and net radiation

Missing G observations were gapfilled by establishing a linear relationship with R_n on a daily basis, relating the resulting slope and intercept parameters with canopy height, and gapfilling using regression parameters that varied as a function of canopy height. If measured R_n data were not available from either tower, a linear relationship for each day between tower R_n and SW_{in} from the Moccasin SCAN site was established and used for gapfilling R_n, which in turn was used to gapfill G.

2.3.2. Gapfilling carbon dioxide flux

Our gapfilling model for F_c needed to simultaneously account for photosynthetic and respiratory processes due to rapid changes in canopy biomass during the growth period and for non-vegetated conditions before plant growth and after harvest. To gapfill F_c, a rectangular hyperbolic model for ecosystem production and the respiration model of Lloyd and Taylor (1994) were combined:

$$F_c = -\frac{\alpha\beta SW_{in}}{\alpha SW_{in}+\beta} + R_{10}exp\left(E_0\left(\frac{1}{T_{10}-T_t}-\frac{1}{T_a-T_t}\right)\right) \quad (1)$$

where α is the initial response of the light response curve (μmol CO_2 J^{-1}), β is gross ecosystem productivity (*GEP*) at light saturation (μmol CO_2 $m^{-2}\,s^{-1}$), R_{10} (μmol CO_2 $m^{-2}\,s^{-1}$) is ecosystem respiration (*RE*) at a T_a of 10 °C (T_{10}), E_0 is the activation energy parameter (K), and the reference temperature T_t is set to 227.13 K following Falge et al. (2001b). Parameters were fit using least squares regression for observations within a seven-day moving window of F_c, SW_{in}, and T_a observations. Parameter sets during periods for which the parameter estimation routine did not converge to an optimal solution or for which observations were not available were estimated using the previous day's values for the case of small gaps of two days or less, and using linear interpolation of parameter values from preceding and subsequent periods for large gaps of more than two days.

2.3.3. Gapfilling latent heat flux

Evapotranspiration (*ET*) was calculated as *LE* divided by the latent heat of vaporization with units set to equal mm per half hour eddy covariance measurement period. Missing *LE* (and thereby *ET*) observations, including those that exceeded logical bounds of $-100\,W\,m^{-2}$ and $600\,W\,m^{-2}$, were gapfilled using the Priestley-Taylor model (Priestley and Taylor, 1972) adjusted to include an uncertainty term, ε_{PT}, that functions as an intercept parameter:

$$ET_0 = \frac{1s(R_n-G)}{\lambda \quad s+\gamma}\alpha_{PT}+\varepsilon_{PT}. \quad (2)$$

Here, λ is the latent heat of vaporization, s is the slope of the saturation vapor pressure-temperature relationship, γ is the psychrometric constant, and α_{PT} is the Priestley-Taylor coefficient. α_{PT} and ε_{PT} were determined for the winter wheat, spring wheat, and fallow fields individually for each day of the study period using linear regression against measured *ET*. α_{PT} and ε_{PT} for days during which insufficient data were available were estimated using the previous day's parameters for the case of small gaps of two days or less, and linear interpolation from the parameters of preceding and subsequent periods for large gaps of more than two days.

2.3.4. Gapfilling sensible heat flux

Missing *H* values, including those that exceeded logical bounds of $-100\,W\,m^{-2}$ and $500\,W\,m^{-2}$, were gapfilled by fitting a daily linear regression between observed *H* and R_n. The linear model included a slope and an intercept parameter similar to equation 2, and missing *H* values were filled using the results of this regression. As with the other flux gapfilling routines, parameters which were unable to be calculated due to missing data were estimated using the previous day's parameters for the case of small gaps of two days or less, and linear interpolation from the parameters of preceding and subsequent periods for large gaps of more than two days.

2.4. Uncertainty analysis

Uncertainty in eddy covariance observations is often on the order of 10–15% (e.g. Goulden et al., 1997), and varies as a function of flux magnitude (Richardson et al., 2008, 2006). The total uncertainty in eddy covariance measurements is a function of observational uncertainty (Moncrieff et al., 1996), gapfilling uncertainty (Falge et al., 2001a, 2001b), and spatial uncertainty due to the assumption that a spatially variable flux can be expressed as an average on a square meter basis (Oren et al., 2006).

We applied the approach of Richardson et al. (2008) to estimate the random uncertainty of F_c, *LE*, and *H*. Briefly, data from the same half hour period of consecutive days were screened for similar micrometeorological conditions defined as those for which R_n differed by less than $75\,W\,m^{-2}$, air temperature differed by less than 3 °C, and average wind speed differed by less than $1\,m\,s^{-1}$ under the assumption that fluxes measured during these conditions on consecutive days should be similar and any differences are related to the random error of eddy covariance measurements. Differences in F_c, *LE*, and *H* identified using this approach were found to be linearly related to the mean flux (Richardson et al., 2008, 2006), the model for which is taken to be the random uncertainty of the flux measurements. Random uncertainty of the seasonal sums of F_c, *LE*, and *H* was taken to be the mean absolute value of these fluxes multiplied by the percent random uncertainty following Stoy et al. (2006a,b).

Random uncertainty was propagated through the gapfilling routines following the recommendations of Motulsky and Ransnas (1987) by perturbing the input flux observations with a random value drawn from a normal distribution multiplied by the random uncertainty calculated using the Richardson et al. (2008) routine. This procedure was repeated 100 times for each day of observations, and 100 parameter sets for the gapfilling model were subsequently fit for each day using least squares regression. Each of the corresponding parameter sets for the case of F_c were tested for convergence of the optimization routine, and all parameter sets were adjusted for missing values using the routines for large and small gaps described above. Gapfilling uncertainty was then determined as the standard deviation of the April–September seasonal flux sum. Total uncertainty for each flux over the study periods was calculated by summing the variance attributable to random uncertainty and that attributable to gapfilling parameter uncertainty – noting the propagation of random error into the estimate of gapfilling uncertainty – in order to obtain a conservative value of total flux uncertainty for each field for each study period.

2.5. Energy balance

The surface-atmosphere energy balance is rarely closed using the eddy covariance and micrometeorological measurements of R_n, *G*, *LE*, and *H* at a single tower (Franssen et al., 2010; Stoy et al., 2013; Wilson et al., 2002), although 26 of the 173 tower sites studied by Stoy et al. (2013) had an energy balance closure greater than 100%. Energy balance closure for the winter wheat, spring wheat, and fallow fields was calculated as the percent of the sum of available energy during the April–September study periods (i.e. $R_n - G$) that is realized as the measured sum of sensible and latent heat fluxes ($H+\lambda E$), excluding periods for which turbulent fluxes were gapfilled.

2.6. Atmospheric boundary layer height model

We used surface-atmosphere exchange observations and a simple one-dimensional *ABL* model to test the conceptual model of Gameda et al. (2007), which assumes that fallow results in *h* on the order of 2–3 km and vegetated surfaces result in *h* on the order of 500 m in the Canadian Prairies. *h* was modeled for each of the management practices following Luyssaert et al. (2014):

$$\Delta h = H_v \Delta t)/\rho_a c_p h\gamma_v) \quad (3)$$

where Δh is the change in h in meters per unit time (Δt), ρ_a is the air density in kg m^{-3}, c_p is the specific heat capacity in J kg^{-1} K^{-1}, γ_v is the virtual temperature inversion strength in K m^{-1} set to 0.003 K m^{-1}, and H_v is the virtual heat flux in W m^{-2} obtained by measured H and LE:

$$H_v = H + 0.07LE. \quad (4)$$

Eq. (3) was calculated for each day during the study periods and h was set to 150 m at the beginning of each day, also following Luyssaert et al. (2014). We focus our comparisons on model predictions of maximum daily h for the different agricultural treatments.

Modeled h is compared to the modeled height of the lifted condensation level (h_{LCL}), which was calculated by dry-adiabatically raising an air parcel with near-surface temperature and moisture to its saturation point approximated by (Stull, 2012):

$$T_{LCL} = \frac{2840}{3.5ln(T_a) - ln\left(\frac{Pr}{0.622+r}\right) - 7.108} + 55 \quad (5)$$

with atmospheric pressure at the surface (P) in kPa, the mixing ratio r, and T_a in K. We focus our discussion of h and h_{LCL} on the 2014 growing season when spring wheat was measured by the first tower and fallow was measured by the second tower.

3. Results

3.1. Prevailing weather conditions

On average, 2014 was cooler, cloudier, and wetter than 2013. Mean annual T_a during 2013 was 7.0 °C and mean April-September T_a was 14.3 °C. Mean annual T_a (6.5 °C) and April–September mean T_a (13.7 °C) were about 0.5 °C cooler in 2014 than 2013. Annual cumulative SW_{in} was 3% greater in 2013 (5290 MJ m^{-2} year^{-1}) than in 2014 (5140 MJ m^{-2} year^{-1}), and the April-September cumulative incident SW_{in} was 5% greater in 2013. Cumulative precipitation measured at the Moccasin SCAN site was 452 mm in 2013 and 503 mm in 2014. The study period cumulative precipitation was 360 mm in 2013 and 391 mm in 2014, 162 mm of which fell during a large precipitation event during Aug. 21–24 shortly after the harvest of the spring wheat field on Aug. 18, 2014.

3.2. Plant height growth

Canopy height was near zero after the 2012 fallow growing season that preceded winter wheat planting. Measureable winter wheat growth began in early May 2013 (Fig. 3). The winter wheat crop reached its maximum height of 0.64 m on July 9, 2013. The canopy was reduced to stubble measured at 0.2 m after harvest on August 7, 2013. With the exception of variation due to snow cover, the plant canopy remained at 0.2 m during the 2013/2014 winter, and was effectively 0 m after spring wheat planting on May 2, 2014. Measurable spring wheat crop growth began on May 26 and reached 0.83 m on July 25, *ca.* two weeks after winter wheat reached its maximum height in 2013. Canopy height was likewise was reduced to 0.2 m stubble after harvest on Aug. 18, 2014 (Fig. 3).

3.3. u^* Thresholds and data availability

The Reichstein et al. (2005) algorithm selects a unique u^* threshold for three month periods, which correspond to April through June and July through September during the study period. The identified u^* thresholds were 0.077 m s^{-1} for 2013 winter wheat, 0.048 m s^{-1} for 2014 spring wheat, and 0.073 m s^{-1} for the fallow field during the April through June period, and 0.054 m s^{-1} for 2013 winter wheat, 0.092 m s^{-1} for 2014 spring wheat, and 0.057 m s^{-1} for the fallow field during the July through September period. Turbulent flux observations taken during periods where measured u^* was less than these values during nighttime were removed from the observational record and filled using the gapfilling procedures described in Sections 2.3.2–2.3.4. The percent of missing data for each treatment that resulted from the u^* filter and logical filters, as well as power system and instrumental failures, is described in Table 3. Uncertainty in flux sums that result from missing data is propagated through the data gapfilling routines to result in monthly and seasonal uncertainty estimates as described in Section 2.4.

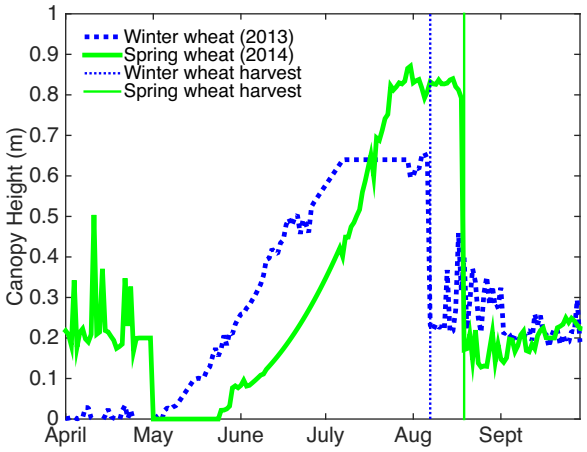

Fig. 3. The daily maximum canopy height or snowpack height for the winter wheat and spring wheat rotations measured by a sonic distance sensor (Table 2). Canopy height was assumed to be near zero before winter wheat growth began in earnest in early May, 2013. Stubble left on the winter wheat field in 2013 measured *ca.* 0.2 m, and was assumed to drop to 0 m following the planting of spring wheat on May 2, 2014.

3.4. Carbon dioxide fluxes

The cumulative sum of F_c in units of carbon in CO_2 (C—CO_2) in all fields during the study period is shown in Fig. 4A. The 2013 winter wheat field became a net sink of carbon (since April 1, 2013) around May 8, 2013, and the 2014 spring wheat field became a net sink of carbon (since April 1, 2014) around May 23, 2014. The winter wheat field had a cumulative C—CO_2 uptake of -208 ± 53 g C m^{-2} during the 2013 April – September study period (expressed as the mean of the gapfilling model simulations plus or minus one standard deviation of random plus gapfilling uncertainty), and the spring wheat field took up -107 ± 29 g C m^{-2} during the 2014 study period (Fig. 4B). The fallow field lost 135 ± 73 g C—CO_2 to the atmosphere during the 2014 study period with two brief periods of net C—CO_2 uptake of *ca.* 10–20 g C m^{-2} corresponding to periods of weedy growth near the tower during late June and weedy growth following the large rain event after the spring wheat harvest in August. The larger uncertainty for F_c in the fallow field is attributable to greater uncertainty in net respiratory

Table 3
The percent of available turbulent flux data during the entire April–September study period for each study site. Daytime refers to periods when the solar zenith angle was less than 90°.

Site	Period	F_c	LE	H
Winter wheat (2013)	Daytime	52%	52%	53%
	Total	48%	49%	49%
Spring wheat (2014)	Daytime	48%	48%	48%
	Total	45%	45%	45%
Fallow (2014)	Daytime	44%	50%	51%
	Total	42%	49%	50%

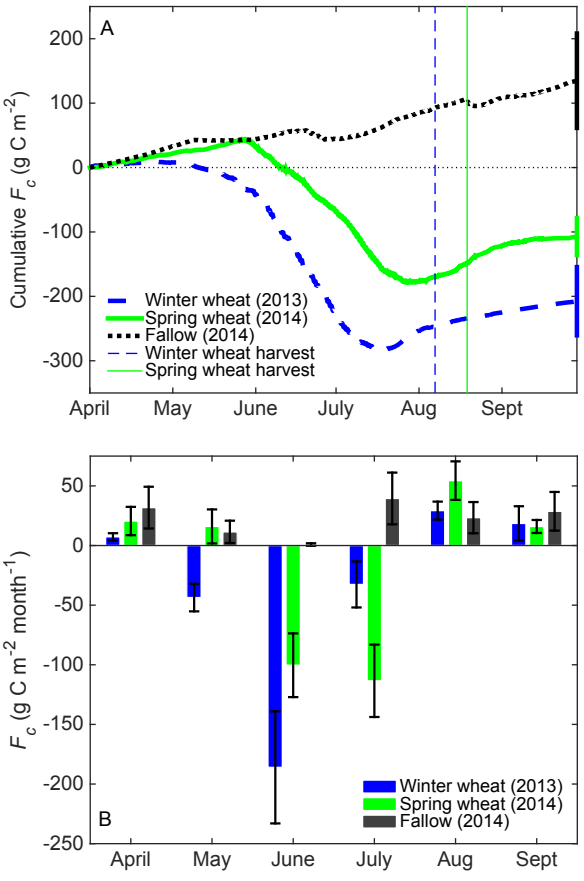

Fig. 4. The cumulative (A) and monthly (B) sums of the net ecosystem exchange of carbon in CO_2 (F_c) between the winter wheat, spring wheat, and fallow fields and the atmosphere during the April-September study period. Negative values denote carbon uptake by the biosphere. Error bars represent one standard deviation from the cumulative or monthly sum.

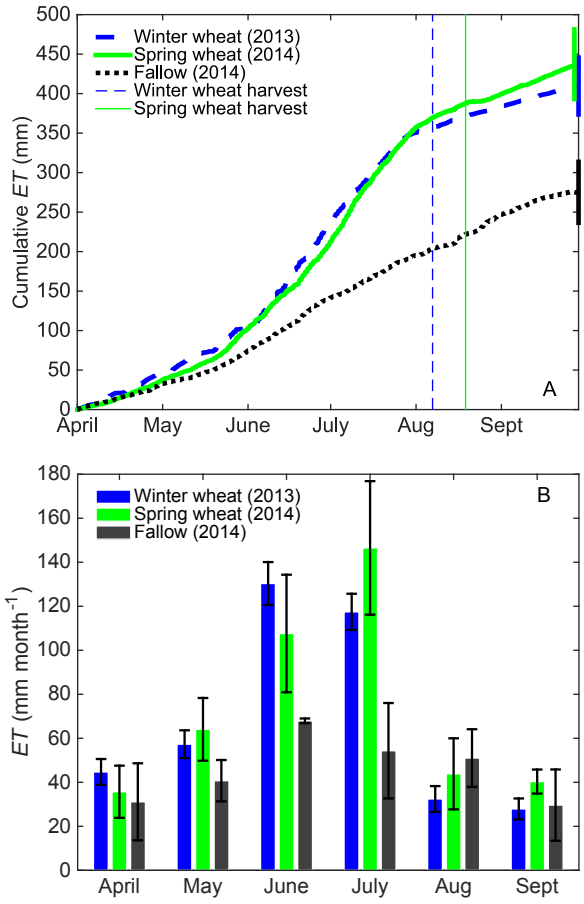

Fig. 5. The cumulative (A) and monthly (B) sums of evapotranspiration (ET) from the winter wheat, spring wheat, and fallow study fields during the the April–September study periods. Error bars represent one standard deviation from the cumulative or monthly sum.

fluxes calculated by the Richardson et al. (2008) algorithm, and the larger uncertainty in F_c at the winter wheat field *versus* the spring wheat field is due in part to the larger uncertainties attributable to larger average flux magnitude.

Maximum monthly F_c occurred at the winter wheat field in June at -186 ± 47 g C—CO_2 month^{-1} (Fig. 4B) and in July at the spring wheat field at -113 ± 30 g C—CO_2 month^{-1}, which is of greater magnitude than F_c in June at the spring wheat field at -100 ± 27 g C—CO_2 month^{-1} as identified by a two-sided *t*-test ($p < 0.05$, Fig. 4B). Monthly F_c from the fallow field peaked in July at 39 ± 22 g C—CO_2 month^{-1}.

3.5. Evapotranspiration

Cumulative *ET* from the 2013 winter wheat field was 410 ± 36 mm during the study period (Fig. 5A), significantly less than the 437 ± 44 mm observed for the 2014 spring wheat field during the cooler and wetter 2014 ($p < 0.05$), but only by some 6% and reflective of the differences in April-September precipitation observed between years. The rate of increase in cumulative *ET* in the 2014 fallow field was not as steep as that in the winter wheat and spring wheat fields, and the Apr.–Sept. total reached 275 ± 39 mm, *ca.* 2/3 of observed *ET* from the spring wheat field. Monthly total *ET* from the winter wheat field peaked in June at 130 ± 10 mm and monthly total *ET* from the spring wheat field peaked in July at 147 ± 10 mm (Fig. 5B), mirroring the monthly patterns of F_c uptake (Fig. 4B). Monthly total *ET* in the Fallow treatment peaked in June and July at *ca.* 69 ± 10 mm.

3.6. Sensible heat fluxes and energy balance closure

H for all treatments before 2013 winter wheat and 2014 spring wheat growth began was similar at *ca.* 2.5 MJ m^{-2} day^{-1}. After crop growth initiated, the increase in cumulative *H* diverged between the spring wheat and fallow fields (Fig. 6A). The winter wheat and spring wheat fields had similar totals of *H* of 445 ± 66 and 465 ± 67 MJ m^{-2} for the respective study periods. *H* at the fallow field reached 759 ± 98 MJ m^{-2} for the study period, an increase in *H* proportional to the decrease in *ET* (Figs. Fig. 5 5A and Fig. 6 6A). Monthly *H* was greater at the fallow field than the wheat fields until harvest in August, especially from the winter wheat field which ceased growth and was harvested sooner than the spring wheat field (see e.g. Fig. 6B). Energy balance closure during the study period was calculated to be 86% at the winter wheat field, 105% at the spring wheat field, and 107% at the fallow field.

3.7. Modeled atmospheric boundary layer height and lifted condensation level

Modeled *h* using surface flux data from the spring wheat and fallow fields that were both measured in 2014 (Fig. 7A) demonstrates a seasonal pattern that follows the seasonal trend in *H* (Fig. 6B), which is the largest contributor to H_v (Eq. (4)). Maximum modeled *h* was 2070 m for the spring wheat field and 2440 m for the fallow field (Fig. 7A), and the maximum daily difference between the two fields was over 900 m (Fig. 7B). The mean difference in modeled maximum daily *h* between the spring wheat

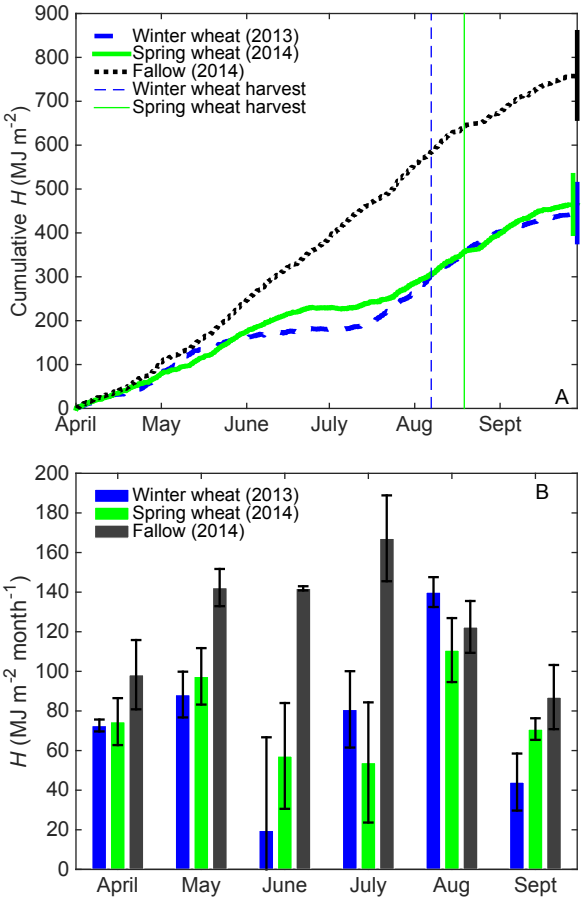

Fig. 6. The cumulative (A) and monthly (B) sums of sensible heat flux (H) from the winter wheat, spring wheat, and fallow study fields during the the April–September study periods. Error bars represent one standard deviation from the cumulative or monthly sum.

and fallow fields was 210 m during the April–September study period.

Differences in modeled h_{LCL} between fallow and spring wheat were minor and averaged 20 m over the study period. As a consequence, h_{LCL} modeled using data from the spring wheat and fallow fields were averaged for subsequent analyses. The mean value of maximum daily h_{LCL} was *ca.* 1600 m but exceeded 3500 m during the month before the spring wheat harvest (Fig. 7A). A comparison of modeled h and h_{LCL} for both spring wheat and fallow indicates that the growing convective ABL height reaches the LCL ($h > h_{LCL}$) on average some 30 min earlier for fallow, and such crossings occurred during 81 days with fallow and 74 days with spring wheat (Fig. 8).

4. Discussion

It is important to recall that the 2014 study period was cooler and wetter than 2013 and comparisons between the winter wheat field (measured in 2013) and the spring wheat and fallow fields (measured in 2014) are subject to these differences in prevailing weather conditions. We first discuss differences in surface-atmosphere carbon dioxide exchange with a focus on the winter wheat and spring wheat fields – noting that the fallow field lost carbon to the atmosphere as expected – followed by an analysis of the impacts of spring wheat *versus* fallow management on the turbulent fluxes of latent and sensible heat and consequences for modeled atmospheric boundary layer development.

4.1. Carbon dioxide exchange

The spring wheat and fallow fields – both measured during 2014 – lost a similar amount of C—CO_2 during April and May before crop growth and during initial stages of spring wheat emergence as quantified as measureable height growth by the sonic distance sensor (Fig. 2; 37 g C m^{-2} for April and May for the spring wheat field and 43 g C m^{-2} for April and May for the fallow field). Mean T_a (8.2 °C) and soil temperature (9.0 °C in the spring wheat field and 9.1 °C in the fallow field) were characteristically low during this period, and carbon fluxes during the largely fallow period in both fields behaved in a similar manner. Following crop emergence, the spring wheat field turned into a net carbon sink (since April 1, 2014) in mid-June. Outside of brief periods of weedy growth, the consistent C source from the fallow field resulted in net April-September C—CO_2 losses (135 ± 73 g C m^{-2} study period^{-1}) that were of similar magnitude to C sinks in the spring wheat field (-107 ± 29 g C m^{-2} study period^{-1}).

Both wheat fields were a net sink of C—CO_2 during the study period on the order of 200 g C m^{-2} for the winter wheat field and 100 g C m^{-2} for the spring wheat field. It has been suggested that non-woody C_3-dominated ecosystems should have similar net ecosystem productivity due to metabolic and organism size constraints (Peichl et al., 2013), bringing into question why the winter wheat field had two-fold greater C—CO_2 uptake than the spring wheat field, especially when canopy height growth was greater in the spring wheat field than the winter wheat field (Fig. 3). Potential explanations include 1) differences in climatological variables between growing seasons; 2) net C—CO_2 efflux in the spring wheat field during April and May after planting (i.e. the difference among fields during the April-September study period is a result of planting date); or 3) respiratory losses from organic matter left from winter wheat field in the spring wheat field noting that chemical fallow preceded winter wheat. We briefly discuss each sequentially.

To test the effects of the cooler and wetter conditions on determining 2014 fluxes, we parameterized the daily F_c model using 2014 flux and micrometeorological observations and forced it with 2013 SW_{in} and T_a observations. This analysis follows the approach of Richardson et al. (2007) to interpret the role of climate *versus* biological and management responses to climate variability of surface-atmosphere fluxes. The cumulative sum of F_c during the study period using the 2014 models forced by 2013 meteorology was -120 g C—CO_2 m^{-2}, a difference of only a *ca.* 10 g C—CO_2 m^{-2} for the study period, suggesting that differences in F_c are not primarily due to differences in growing season climate.

The second explanation – differences in crop emergence timing – contributes to the differences in CO_2 uptake between the winter wheat and spring wheat crops. The spring wheat field lost *ca.* 40 g C m^{-2} during April and May before the spring wheat field became a net daily sink for C—CO_2 around May 29, 2014. Due to earlier planting and thereby crop emergence, the winter wheat field became a net C—CO_2 sink at the beginning of May. Differences in seasonal F_c even among winter wheat treatments has been attributed to differences in early season crop development (Dufranne et al., 2011).

The third explanation – that there is a greater respiratory source in the spring wheat field – can be confirmed by analyzing the parameters of the gapfilling model (Eq. (1)). The mean R_{10} parameter during the period of peak growth in the winter wheat field is *ca.* 2.5 μmol CO_2 m^{-2} s^{-1}, but over 3 μmol CO_2 m^{-2} s^{-1} in the spring wheat field. Using mean R_{10} and E_0 parameters in the respiratory component of Eq. (1) with observed T_a – noting that Eq. (1) is designed to gapfill F_c rather than partition it into its components (Reichstein et al., 2012; Wehr et al., 2016) – results in a modeled RE of 263 g C m^{-2} during the study period in the winter

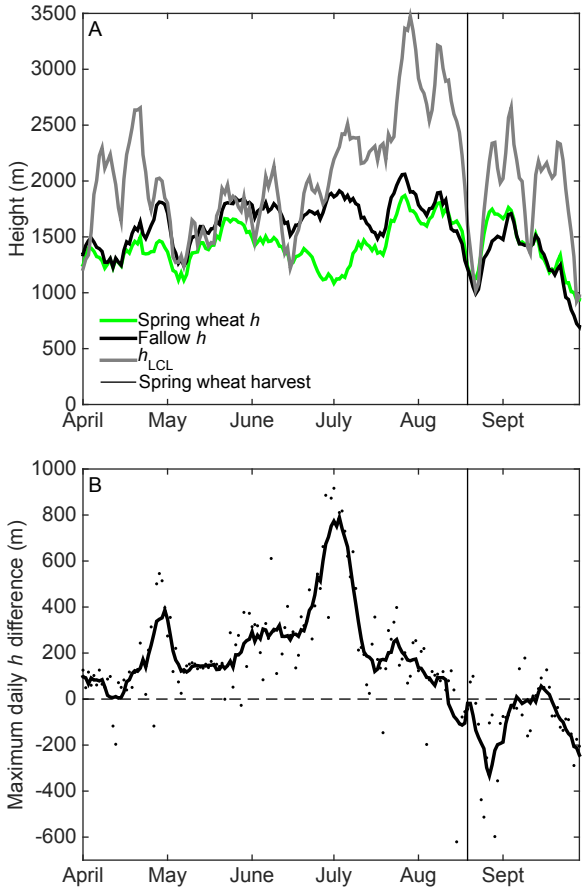

Fig. 7. (A) The maximum daily height of the modeled atmospheric boundary layer (h) calculated using surface virtual heat flux measurements from the spring wheat and fallow fields and a one dimensional boundary layer model following Luyssaert et al. (2014) (Eq. (3)) and the height of the lifted condensation level (h_{LCL}) for maximum daily air temperature modeled by lifting air parcels dry adiabatically to the saturation point temperature (Eq. (5)) using meteorological observations from 2014 from the spring wheat and fallow study sites. Daily values were smoothed using a seven-day digital filter. (B) The difference in simulated h among the spring wheat and fallow fields. Dots represent daily maximum modeled h and lines represent the output of a seven day digital filter.

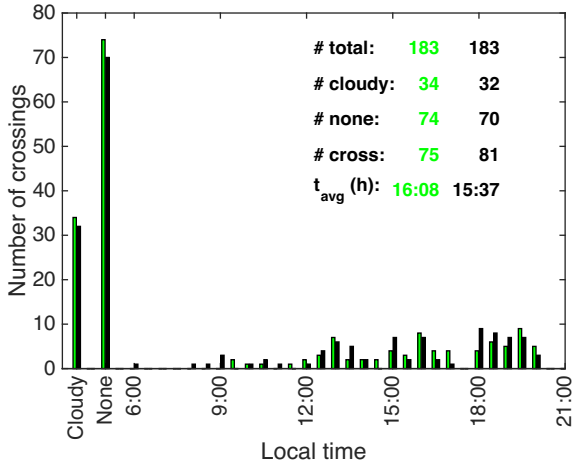

Fig. 8. Histogram of times during the April–September 2014 study period when modeled daytime lifted condensation level (h_{LCL}) first exceeds the height of the atmospheric boundary layer (h). 'None' and 'cloudy' refers to days when daytime h_{LCL} never exceeds h and when h_{LCL} at sunrise was below 150 m, respectively.

wheat field and 488 g C m^{-2} during the study period in the spring wheat field. This difference may seem large, but using these modeled *RE* values to model *GEP* as the difference between F_c and *RE* results in −466 g C m^{-2} during the study period in the winter wheat field and −595 g C m^{-2} in the spring wheat field, a difference of about 25% that is proportional to the difference in maximum canopy height (Fig. 3). Greater *GEP* in the spring wheat field results in more labile C available for *RE* (Högberg et al., 2001; Ryan and Law, 2005; Stoy et al., 2007), but differences in modeled *RE* are greater than differences in *GEP* among fields, pointing to a respiratory source in the spring wheat field that is not present in the winter wheat field. These results are consistent with the findings of Schmidt et al. (2012) and Waldo et al. (2016), who demonstrated the importance of plant residues from previous crops to the crop carbon balance. The plant residues that were left after the 2013 winter wheat harvest (e.g. Fig. 3) that remained in the field during the 2014 spring wheat crop – noting that chemical fallow preceded winter wheat – cannot be excluded as a cause of the differences in C—CO_2 uptake between our winter wheat and spring wheat observations. These findings are in agreement with the findings of Peichl et al. (2013) in that differences in carbon metabolism in these non-woody C_3 systems was dominated by the impacts of land management.

4.2. Evapotranspiration and water management

Daily *ET* sums quantified here are similar to or greater than other studies in wheat cropping systems. Maximum daily *ET* was *ca.* 7 mm day^{-1} for the winter wheat crop (in June) and the spring wheat crop (in July), which corresponds to low surface resistance to water by wheat (Bonan, 2008) during periods with sufficient soil moisture and the high incident radiation load of the study sites. That being said, the maximum value of α_{PT} calculated by the gapfilling models was 0.75 for winter wheat and 0.85 for spring wheat, far less than the theoretical maximum of 1.26 described by Priestley and Taylor (1972) and values found for irrigated wheat crops (e.g. 1.17–1.26; Zhang et al., 2004), suggesting limitations to the transport of water between soil and atmosphere that may be due to either stomatal closure or limited evaporation due to dry soil surface conditions. Future work should seek to identify the source of this water limitation, perhaps using advanced algorithms for estimating the contribution of evaporation and transpiration to *ET* using high frequency eddy covariance data (Scanlon and Kustas, 2010; Scanlon and Sahu, 2008; Sulman et al., 2016).

There were notable differences amongst *ET* observed here and in other wheat cropping systems. Anthoni et al. (2004a,b) found maximum rates of *ET* on the order 3–4 mm day^{-1} in mid-May in a winter wheat crop in Germany, far lower than the 7 mm day^{-1} maximum observed here. We can estimate SW_{in} from *PPFD* observations at the Gebesee study site of Anthoni et al. (2004a, b) and approximate annual SW_{in} to be on the order of 3500–4010 MJ m^{-2} year^{-1}, which is approximately 2/3 of the annual SW_{in} received by the Judith Basin study sites. In other words, differences in maximum *ET* among our observations and those of Anthoni et al. (2004a,b) are due in part to lower SW_{in} during the growing season in central Europe.

ET was predictably higher in the winter wheat and spring wheat fields than the fallow field (Fig. 5A), confirming that fallowing results in soil water savings if lateral water transport and drainage losses can be assumed to be minimal during the growth period. Winter wheat *ET* was 410 mm during the April–September study period, which represented *ca.* 90% of the total precipitation based on the data from the Moccasin SCAN site in 2013 for the same time frame, noting that precipitation maps suggest that the study fields receive slightly more precipitation than the Moccasin SCAN site on average due to topographical influences. Total *ET* for the spring

wheat and fallow fields during the 2014 study period was 440 mm and 315 mm, which was *ca.* 90% and 60% respectively of Moccasin SCAN precipitation observations in 2014. In other words, wheat cropping returned almost all incident precipitation to the atmosphere, while the fallow field left over 100 mm of water available for a subsequent crop, or for deep drainage.

It is likely that the no-till treatment reduced *ET* in the fallow field *versus* a situation in which it was tilled; Chi et al. (2016) for example demonstrated that tillage tended to increase soil evaporation. It is important to note that *ET* may be underestimated in the winter wheat field and overestimated in the spring wheat and fallow fields owing to imperfect energy balance closure, but it is unclear if radiometric or turbulent flux observations are the cause of the imperfect closure and current practices suggest that turbulent flux observations should not be adjusted to match radiometric observations (Baldocchi, 2008).

The amount of water that would need to be replenished to equal the water savings conferred by fallow during the study period is on the order of 100 mm. Stubble height in our case is 0.2 m (Fig. 3), and snow tended to accumulate to stubble height in the study fields. If we assume a characteristic snow density in MT to be on the order of 0.08 g cm^{-3} (Jacobson, 2010; Welch et al., 2016), the depth of water that corresponds to 0.2 m of snow of this density is 16 mm of water, an order of magnitude less than the amount of water that needs to be replenished to account for water use of the wheat fields. In other words, changes in stubble management are unlikely to make up the difference in water lost to the atmosphere among the wheat and fallow fields. If water in the soil column during the non-growing season is replenished such that soil moisture is at or near field capacity before crop growth regardless of prior agricultural treatment, the water savings benefits of fallow should be questioned.

4.3. Impacts of surface conditions on atmospheric boundary layer & lifted condensation level

Cumulative H at both wheat fields was *ca.* 450 MJ m^{-2} during the study period, with important seasonal differences due to crop development and harvest that have implications for energy inputs into the *ABL* and its diurnal growth (Fig. 7A). The choice to fallow is among these management decisions with implications for *ABL* dynamics as evidenced by large differences in modeled maximum daily h between the spring wheat and fallow fields, especially during the peak crop growth period in June and July in our case (Fig. 7B).

Gameda et al. (2007) studied the impacts of fallow reduction on regional climate in the Canadian Prairie Provinces and used a conceptual model to argue that fallow results in (modeled) h on the order of 2–3 km but h resulting from vegetated surfaces is on the order of 0.5 km. Their reasoning is that R_n in fallow is greater due to lower albedo and is preferentially partitioned into H, which results in greater virtual heat flux following Eq. (4), while vegetated surfaces partition R_n preferentially into *LE* resulting in a cooler and shallower *ABL*. Fig. 7A agrees with Gameda et al. (2007) in that the modeled h is higher as a result of observed surface fluxes from the fallow field *versus* the spring wheat field, but our results differ in magnitude. Our results suggest that the conceptual model of Gameda et al. (2007) underestimates h in wheat scenarios. It is important to note that the one-dimensional simulations presented here simply estimate the influence of a single surface (spring wheat *versus* fallow) on a modeled vertical column of the atmosphere and do not seek to simulate realistic atmospheric flows.

The intersection of the convective *ABL* height with the *LCL* is a necessary, albeit not sufficient, condition for the initiation of local convection (e.g. Juang et al., 2007a; Juang et al., 2007b). Maximum daily h_{LCL} differed on average by *ca.* 20 m between the two plots, which can be explained by their close proximity. Low relative humitidies and hot air temperatures during the month preceding spring wheat harvest led to modeled h_{LCL} greater than 2500 m, which exceeded maximum h and suggests that convective precipitation during this period is unlikely. There was a tendency to reach h_{LCL} sooner and more often in the fallow simulation due to higher H and thus h above fallow, (Fig. 8). These findings, however, need to be interpreted with caution for two reasons. (i) Differences in surface meteorology between the experimental plots are small, and (ii) h as well as h_{LCL} are calculated from local quantities, which do not account for feedbacks between the regional surface energy balance and the thermodynamic state of the atmosphere as well as non-local effects such as the development of mesoscale circulations between patches with different surface characteristics (e.g. Taylor et al., 2007).

Overall, large-scale reduction of fallow has the potential to decrease h by several hundred meters. Similarly, Betts et al. (2013b) found that there was a systematic reduction in h_{LCL} in the Canadian Prairies of approximately 200 m from 1953 to 2011, which is similar to the calculated mean change in h of 210 m, highlighting the uncertain nature of the net effect on convective development. h and h_{LCL} have more crossings in the fallow simulation yet fallow reduction is thought to result in an increase in cloud development and convective initiation. Our results suggest that studies of the effects of fallow on near-surface temperature and humidity following Betts et al. (2013b) should be extended to the regions of fallow reduction in the U.S. to ascertain how land use changes across the entire northern North American Great Plains has impacted regional climate.

The details of the differences – and similarities – among modeled h and h_{LCL} as they impact cloud formation processes and convective precipitation over wheat growing areas has yet to be ascertained. Given the reduction in the practice of fallow over the past four decades on the order of tens of millions of hectares (Fig. 1), the role of cropping systems and planting decisions needs to be further investigated to quantify the proposed role of agricultural management in the observed summertime cooling trend and increase in precipitation across parts of the northern North American Great Plains (Betts et al., 2013a, 2013b; Mahmood et al., 2014). Future research should study the impacts of management patterns in space and time on h and h_{LCL} dynamics – and measurements of h should be made or estimated from radiosonde data (e.g. Seidel et al., 2010) – to understand the consequences of land management across the northern North American Great Plains on atmospheric dynamics of importance to convective precipitation.

5. Conclusions

Greater CO_2 uptake by the winter wheat field (*ca.* −200 g C m^{-2}) than the spring wheat (*ca.* −100 g C m^{-2}) field during the April–September study period were largely due to the effects of ecosystem management: Carbon losses in April and May from the spring wheat field combined with a larger respiratory source during the main growth period – consistent with the respiration of residues from the previous winter wheat crop – explain most of the difference in F_c among the wheat fields. CO_2 losses from the wheat fields before plant emergence and after harvest occur at a similar rate as CO_2 losses from the fallow field, which represented a total C—CO_2 loss to the atmosphere of over 100 g C m^{-2} during the April–September study period. Total April–September *ET* was similar between the winter wheat and spring wheat fields despite differences in prevailing climatic conditions and crop emergence and harvest dates, suggesting that ecosystem water use efficiency was greater in the winter wheat field with greater F_c. Cropping

systems management also had important implications for *H* and thereby *ABL* dynamics, the maximum daily value of which was *ca.* 200 m less in spring wheat *versus* fallow simulations, which is on the order of the reduction of h_{LCL} demonstrated by Betts et al. (2013b) from the period 1951–1991 to 1992–2011. Future research should quantify the amount of *ET* resulting from evaporation and transpiration to understand sources of water to the atmosphere and its interaction with plant water use and growth, and investigate the implications of widespread changes in agricultural management in the northern North American Great Plains – including alternate cropping sequences – on regional climatology.

Acknowledgements

This work was supported by the Montana Wheat and Barley Committee, the Montana University System Water Center, the USDA National Institute of Food and Agriculture Hatch project 228396, and NSF DEB 1552976 'The role of ecosystem management on boundary layer development and precipitation in the Northern Plains'. We would like to thank Adam Sigler, Simon Fordyce, Aiden Johnson, Robby Robertson, and Dr. Lin Hua for field assistance and coordination and David Walker for advice on agricultural statistics. We would also like to thank the landowner Bob Otten and the farm operator Brandon Morris for permission, coordination, and invaluable insight. Stephanie Ewing, Perry Miller, and Rob Payn provided valuable comments on the manuscript and Clain Jones and Adam Sigler provided valuable information on soil characteristics.

References

Anthoni, P.M., Freibauer, A., Kolle, O., Schulze, E.-D., 2004a. Winter wheat carbon exchange in Thuringia, Germany. Agric. For. Meteorol. 121, 55–67.

Anthoni, P.M., Knohl, A., Rebmann, C., Freibauer, A., Mund, M., Ziegler, W., Kolle, O., Schulze, E.-D., 2004b. Forest and agricultural land-use-dependent CO2 exchange in Thuringia, Germany. Glob. Change Biol. 10, 2005–2019.

Aubinet, M., Grelle, A., Ibrom, A., Rannik, U., Moncrieff, J., Foken, T., Kowalski, A.S., Martin, P.H., Berbigier, P., Bernhofer, C., Clement, R., Elbers, J., Granier, A., Grunwald, T., Morgenstern, K., Pilegaard, K., Rebmann, C., Snijders, W., Valentini, R., Vesala, T., 2000. Estimates of the annual net carbon and water exchange of forests: the EUROFLUX methodology. Adv. Ecol. Res. 30, 113–175.

Béziat, P., Ceschia, E., Dedieu, G., 2009. Carbon balance of a three crop succession over two cropland sites in South West France. Agric. For. Meteorol. 149, 1628–1645.

Baldocchi, D.D., 2008. Breathing of the terrestrial biosphere: lessons learned from a global network of carbon dioxide flux measurements systems. Turner Rev. Aust. J. Bot. 56, 1–26.

Betts, A.K., Desjardins, R., Worth, D., 2013a. Cloud radiative forcing of the diurnal cycle climate of the Canadian Prairies. J. Geophys. Res. Atmos. 118, 8935–8953.

Betts, A.K., Desjardins, R., Worth, D., Cerkowniak, D., 2013b. Impact of land use change on the diurnal cycle climate of the Canadian Prairies. J. Geophys. Res. Atmos. 118, 11–996.

Billesbach, D.P., Berry, J.A., Seibt, U., Maseyk, K., Torn, M.S., Fischer, M.L., Abu-Naser, M., Campbell, J.E., 2014. Growing season eddy covariance measurements of carbonyl sulfide and CO2 fluxes: COS and CO_2 relationships in Southern Great Plains winter wheat. Agric. For. Meteorol. 184, 48–55.

Bonan, G.B., 2008. Forests and climate change: forcings feedbacks, and the climate benefits of forests. Science (80-.) 320, 1444–1449.

Burgess, M.H., Miller, P.R., Jones, C.A., 2012. Pulse crops improve energy intensity and productivity of cereal production in Montana, USA. J. Sustain. Agric. 36, 699–718.

Buyanovsky, G.A., Wagner, G.H., 1998. Changing role of cultivated land in the global carbon cycle. Biol. Fertil. Soils 27, 242–245.

Chi, J., Waldo, S., Pressley, S., O'Keeffe, P., Huggins, D., Stöckle, C., Pan, W.L., Brooks, E., Lamb, B., 2016. Assessing carbon and water dynamics of no-till and conventional tillage cropping systems in the inland Pacific Northwest US using the eddy covariance method. Agric. For. Meteorol. 218–219, 37–49.

Cihacek, L.J., Ulmer, M.G., 1995. Estimated soil organic carbon losses from long-term crop-fallow in the Northern Great Plains of the USA. Soil Manag. Greenh. Effect 85–92.

Dhuyvetter, K.C., Thompson, C.R., Norwood, C.A., Halvorson, A.D., 1996. Economics of dryland cropping systems in the Great Plains: a review. J. Prod. Agric. 9, 216–222.

Dufranne, D., Moureaux, C., Vancutsem, F., Bodson, B., Aubinet, M., 2011. Comparison of carbon fluxes, growth and productivity of a winter wheat crop in three contrasting growing seasons. Agric. Ecosyst. Environ. 141, 133–142.

Yearbook, FAO Statistical. "World food and agriculture." Food and Agriculture Organization of the United Nations, Rome (2013).

Falge, E., Baldocchi, D., Olson, R., Anthoni, P., Aubinet, M., Bernhofer, C., Burba, G., Ceulemans, R., Clement, R., Dolman, H., Granier, A., Gross, P., Grunwald, T., Hollinger, D., Jensen, N.O., Katul, G., Keronen, P., Kowalski, A., Lai, C.T., Law, B.E., Meyers, T., Moncrieff, J., Moors, E., Munger, J.W., Pilegaard, K., Rannik, U., Rebmann, C., Suyker, A., Tenhunen, J., Tu, K., Verma, S., Vesala, T., Wilson, K., Wofsy, S., 2001a. Gap filling strategies for defensible annual sums of net ecosystem exchange. Agric. For. Meteorol. 107, 43–69.

Falge, E., Baldocchi, D., Olson, R., Anthoni, P., Aubinet, M., Bernhofer, C., Burba, G., Ceulemans, R., Clement, R., Dolman, H., Granier, A., Gross, P., Grunwald, T., Hollinger, D., Jensen, N.O., Katul, G., Keronen, P., Kowalski, A., Lai, C.T., Law, B.E., Meyers, T., Moncrieff, J., Moors, E., Munger, J.W., Pilegaard, K., Rannik, U., Rebmann, C., Suyker, A., Tenhunen, J., Tu, K., Verma, S., Vesala, T., Wilson, K., Wofsy, S., 2001b. Gap filling strategies for long term energy flux data sets. Agric. For. Meteorol. 107, 71–77.

Franssen, H.J.H., Stöckli, R., Lehner, I., Rotenberg, E., Seneviratne, S.I., 2010. Energy balance closure of eddy-covariance data: a multisite analysis for European FLUXNET stations. Agric. For. Meteorol. 150, 1553–1567. doi:http://dx.doi.org/10.1016/j.agrformet.2010.08.005.

Gameda, S., Qian, B., Campbell, C.A., Desjardins, R.L., 2007. Climatic trends associated with summerfallow in the Canadian Prairies. Agric. For. Meteorol. 142, 170–185.

Goulden, M.L., Daube, B.C., Fan, S.-M., Sutton, D.J., Bazzaz, A., Munger, J.W., Wofsy, S. C., 1997. Physiological responses of a black spruce forest to weather. J. Geophys. Res. 102, 28987–28996.

Gu, L.H., Falge, E.M., Boden, T., Baldocchi, D.D., Black, T.A., Saleska, S.R., Suni, T., Verma, S.B., Vesala, T., Wofsy, S.C., Xu, L.K., 2005. Objective threshold determination for nighttime eddy flux filtering. Agric. For. Meteorol. 128, 179–197.

Högberg, P., Nordgren, A., Buchmann, N., Taylor, A.F.S., Ekblad, A., Högberg, M.N., Nyberg, G., Ottoson-Löfvenius, M., Read, D.J., 2001. Large-scale forest girdling shows that current photosynthesis drives soil respiration. Nature 411, 789–792.

Hawkesford, M.J., Araus, J., Park, R., Calderini, D., Miralles, D., Shen, T., Zhang, J., Parry, M.A.J., 2013. Prospects of doubling global wheat yields. Food Energy Secur. 2, 34–48.

IPCC, 2007. Climate Change 2007: the Physical Science Basis. Contribution of Working Group I to the Fourth Assessment Report of the Intergovernmental Panel on Climate Change. Cambridge University Press, Cambridge, United Kingdom and New York, NY, USA.

Ingwersen, J., Steffens, K., Högy, P., Warrach-Sagi, K., Zhunusbayeva, D., Poltoradnev, M., Gäbler, R., Wizemann, H.-D., Fangmeier, A., Wulfmeyer, V., Streck, T., 2011. Comparison of Noah simulations with eddy covariance and soil water measurements at a winter wheat stand. Agric. For. Meteorol. 151, 345–355.

Jacobson, M.D., 2010. Inferring snow water equivalent for a snow-covered ground reflector using GPS multipath signals. Remote Sens. 2, 2426. doi:http://dx.doi.org/10.3390/rs2102426.

Juang, J.-Y., Katul, G.G., Porporato, A., Stoy, P.C., Siqueira, M.S., Detto, M., Kim, H.-S., Oren, R., 2007a. Eco-hydrological controls on summertime convective rainfall triggers. Glob. Change Biol. 887–896.

Juang, J.-Y., Porporato, A., Stoy, P.C., Siqueira, M.B.S., Oishi, A.C., Detto, M., Kim, H.-S., Katul, G.G., 2007b. Hydrologic and atmospheric controls on initiation of convective precipitation events. Water Resour. Res. 43.

Kaimal, J.C., Finnegan, J.J., 1994. Atmospheric Boundary Layer Flows: Their Structure and Measurements. Oxford, New York.

Lloyd, J., Taylor, J.A., 1994. On the temperature dependence of soil respiration. Funct. Ecol. 8, 315–323.

Long, J.A., Lawrence, R.L., Greenwood, M.C., Marshall, L., Miller, P.R., 2013. Object-oriented crop classification using multitemporal ETM+ SLC-off imagery and random forest. GISci. Remote Sens. 50, 418–436.

Long, J.A., Lawrence, R.L., Miller, P.R., Marshall, L.A., Greenwood, M.C., 2014. Adoption of cropping sequences in northeast Montana: a spatio-temporal analysis. Agric. Ecosyst. Environ. 197, 77–87.

Lubowski, R.N., Vesterby, M., Bucholtz, S., Baez, A., Roberts, M.J., 2006. Major Uses of Land in the United States, 2002. Department of Agriculture, Economic Research Service, United States.

Luyssaert, S., Jammet, M., Stoy, P.C., Estel, S., Pongratz, J., Ceschia, E., Churkina, G., Don, A., Erb, K., Ferlicoq, M., Gielen, B., Grunwald, T., Houghton, R.A., Klumpp, K., Knohl, A., Kolb, T., Kuemmerle, T., Laurila, T., Lohila, A., Loustau, D., McGrath, M. J., Meyfroidt, P., Moors, E.J., Naudts, K., Novick, K., Otto, J., Pilegaard, K., Pio, C.A., Rambal, S., Rebmann, C., Ryder, J., Suyker, A.E., Varlagin, A., Wattenbach, M., Dolman, A.J., 2014. Land management and land-cover change have impacts of similar magnitude on surface temperature. Nat. Clim. Change 4, 389–393.

Mahmood, R., Pielke, R.A., Hubbard, K.G., Niyogi, D., Dirmeyer, P.A., McAlpine, C., Carleton, A.M., Hale, R., Gameda, S., Beltrán-Przekurat, A., 2014. Land cover changes and their biogeophysical effects on climate. Int. J. Climatol. 34, 929–953.

Mauder, M., Foken, T., 2004. Documentation and Instruction Manual of the Eddy Covariance Software Package TK2. Univ., Abt. Mikrometeorologie.

Merrill, S.D., Black, A.L., Fryrear, D.W., Saleh, A., Zobeck, T.M., Halvorson, A.D., Tanaka, D.L., 1999. Soil wind erosion hazard of spring wheat?fallow as affected by long-term climate and tillage. Soil Sci. Soc. Am. J. 63, 1768–1777.

Miller, P.R., McConkey, B.G., Clayton, G.W., Brandt, S.A., Staricka, J.A., Johnston, A.M., Lafond, G.P., Schatz, B.G., Baltensperger, D.D., Neill, K.E., 2002. Pulse crop adaptation in the northern Great Plains. Agron. J. 94, 261–272.

Miller, P.R., Gan, Y., McConkey, B.G., McDonald, C.L., 2003. Pulse crops for the northern Great Plains. Agron. J. 95, 980–986.
Moncrieff, J.B., Malhi, Y., Leuning, R., 1996. The propagation of errors in long-term measurements of land-atmosphere fluxes of carbon and water. Glob. Change Biol. 2, 231–240.
Motulsky, H.J., Ransnas, L.A., 1987. Fitting curves to data using nonlinear regression: a practical and nonmathematical review. FASEB J. 1, 365–374.
Moureaux, C., Debacq, A., Hoyaux, J., Suleau, M., Tourneur, D., Vancutsem, F., Bodson, B., Aubinet, M., 2008. Carbon balance assessment of a Belgian winter wheat crop (Triticum aestivum L.). Glob. Change Biol. 14, 1353–1366.
Oren, R., Hsieh, C.I., Stoy, P.C., Albertson, J.D., McCarthy, H.R., Harrell, P., Katul, G.G., 2006. Estimating the uncertainty in annual net ecosystem carbon exchange: spatial variation in turbulent fluxes and sampling errors in eddy-covariance measurements. Glob. Change Biol. 12, 883–896.
Papale, D., Reichstein, M., Aubinet, M., Canfora, E., Bernhofer, C., Kutsch, W., Longdoz, B., Rambal, S., Valentini, R., Vesala, T., Yakir, D., 2006. Towards a standardized processing of Net Ecosystem Exchange measured with eddy covariance technique: algorithms and uncertainty estimation. Biogeosciences 3, 571–583.
Papale, D., 2012. Data gap filling. Eddy Covariance. Springer, pp. 159–172.
Peichl, M., Sonnentag, O., Wohlfahrt, G., Flanagan, L.B., Baldocchi, D.D., Kiely, G., Galvagno, M., Gianelle, D., Marcolla, B., Pio, C., Migliavacca, M., Jones, M.B., Saunders, M., 2013. Convergence of potential net ecosystem production among contrasting C3 grasslands. Ecol. Lett. 16, 502–512.
Priestley, C.H.B., Taylor, R.J., 1972. On the assessment of surface heat flux and evaporation using large-scale parameters. Mon. Weather Rev. 100, 81–92.
Reichstein, M., Falge, E., Baldocchi, D., Papale, D., Aubinet, M., Berbigier, P., Bernhofer, C., Buchmann, N., Gilmanov, T.G., Granier, A., Grünwald, T., Havránková, K., Ilvesniemi, H., Janous, D., Knohl, A., Laurila, T., Lohila, A., Loustau, D., Matteucci, G., Meyers, T., Miglietta, F., Ourcival, J.-M., Pumpanen, J., Rambal, S., Rotenberg, E., Sanz, M., Tenhunen, J., Seufert, G., Vaccari, F., Vesala, T., Yakier, D., Valentini, R., 2005. On the separation of net ecosystem exchange into assimilation and ecosystem respiration: review and improved algorithm. Glob. Change Biol. 11, 1424–1439.
Reichstein, M., Stoy, P.C., Desai, A.R., Lasslop, G., Richardson, A.D., 2012. Partitioning of net fluxes. Eddy Covariance. Springer, pp. 263–289.
Richardson, A.D., Hollinger, D.Y., Burba, G.G., Davis, K.J., Flanagan, L.B., Katul, G.G., Munger, J.W., Ricciuto, D.M., Stoy, P.C., Suyker, A.E., Verma, S.B., Wofsy, S.C., 2006. A multi-site analysis of random error in tower-based measurements of carbon and energy fluxes. Agric. For. Meteorol. 136, 1–18.
Richardson, A.D., Hollinger, D.Y., Aber, J.D., Ollinger, S.V., Braswell, B.H., 2007. Environmental variation is directly responsible for short- but not long-term variation in forest-atmosphere carbon exchange. Glob. Change Biol. 13, 788–803. doi:http://dx.doi.org/10.1111/j.1365-2486.2007.01330.x.
Richardson, A.D., Mahecha, M.D., Falge, E., Kattge, J., Moffat, A.M., Papale, D., Reichstein, M., Stauch, V.J., Braswell, B.H., Churkina, G., Kruijt, B., Hollinger, D.Y., 2008. Statistical properties of random CO_2 flux measurement uncertainty inferred from model residuals. Agric. For. Meteorol. 148, 38–50.
Ryan, M.G., Law, B.E., 2005. Interpreting, measuring, and modeling soil respiration. Biogeochemistry 73, 3–27.
Scanlon, T.M., Kustas, W.P., 2010. Partitioning carbon dioxide and water vapor fluxes using correlation analysis. Agric. For. Meteorol. 150, 89–99.
Scanlon, T.M., Sahu, P., 2008. On the correlation structure of water vapor and carbon dioxide in the atmospheric surface layer: a basis for flux partitioning. Water Resour. Res. 44, W10418.
Schmidt, M., Reichenau, T.G., Fiener, P., Schneider, K., 2012. The carbon budget of a winter wheat field: an eddy covariance analysis of seasonal and inter-annual variability. Agric. For. Meteorol. 165, 114–126.
Seidel, D.J., Ao, C.O., Li, K., 2010. Estimating climatological planetary boundary layer heights from radiosonde observations: comparison of methods and uncertainty analysis. J. Geophys. Res. Atmos. 115, D16113.
Stoy, P.C., Katul, G.G., Siqueira, M.B.S., Juang, J.-Y., McCarthy, H.R., Oishi, A.C., Uebelherr, J.M., Kim, H.-S., Oren, R., 2006a. Separating the effects of climate and vegetation on evapotranspiration along a successional chronosequence in the southeastern U. S. Glob. Change Biol. 12, 2115–2135.
Stoy, P.C., Katul, G.G., Siqueira, M.B.S., Juang, J.-Y., Novick, K.A., Uebelherr, J.M., Oren, R., 2006b. An evaluation of models for partitioning eddy covariance-measured net ecosystem exchange into photosynthesis and respiration. Agric. For. Meteorol. 141, 2–18.
Stoy, P.C., Palmroth, S., Oishi, A.C., Siqueira, M.B.S., Juang, J.-Y., Novick, K.A., Ward, E.J., Katul, G.G., Oren, R., 2007. Are ecosystem carbon inputs and outputs coupled at short time scales? A case study from adjacent pine and hardwood forests using impulse-response analysis. Plant Cell Environ. 30, 700–710.
Stoy, P., Mauder, M., Foken, T., Marcolla, B., Boegh, E., Ibrom, A., Arain, M.A., Arneth, A., Aurela, M., Bernhofer, C., Cescatti, A., Dellwik, E., Duce, P., Gianelle, D., van Gorsel, E., Kiely, G., Knohl, A., Margolis, H., McCaughey, H., Merbold, L., Montagnani, L., Papale, D., Reichstein, M., Saunders, M., Serrano-Ortiz, P., Sottocornola, M., Spano, D., Vaccari, F., Varlagin, A., 2013. A data-driven analysis of energy balance closure across FLUXNET research sites: the role of landscape scale heterogeneity. Agric. For. Meteorol. 171, 137–152.
Stull, R.B., 2012. An Introduction to Boundary Layer Meteorology. Springer Science & Business Media.
Sulman, B.N., Roman, D.T., Scanlon, T.M., Wang, L., Novick, K.A., 2016. Comparing methods for partitioning a decade of carbon dioxide and water vapor fluxes in a temperate forest. Agric. For. Meteorol. 226–227, 229–245.
Sus, O., Williams, M., Bernhofer, C., Béziat, P., Buchmann, N., Ceschia, E., Doherty, R., Eugster, W., Grünwald, T., Kutsch, W., 2010. A linked carbon cycle and crop developmental model: description and evaluation against measurements of carbon fluxes and carbon stocks at several European agricultural sites. Agric. Ecosyst. Environ. 139, 402–418.
Taylor, C.M., Parker, D.J., Harris, P.P., 2007. An observational case study of mesoscale atmospheric circulations induced by soil moisture. Geophys. Res. Lett. 34.
Waldo, S., Chi, J., Pressley, S.N., O'Keeffe, P., Pan, W.L., Brooks, E.S., Huggins, D.R., Stöckle, C.O., Lamb, B.K., 2016. Assessing carbon dynamics at high and low rainfall agricultural sites in the inland Pacific Northwest US using the eddy covariance method. Agric. For. Meteorol. 218–219, 25–36.
Wehr, R., Munger, J.W., McManus, J.B., Nelson, D.D., Zahniser, M.S., Davidson, E.A., Wofsy, S.C., Saleska, S.R., 2016. Seasonality of temperate forest photosynthesis and daytime respiration. Nature 534, 680–683.
Welch, C.M., Stoy, P.C., Rains, F.A., Johnson, A.V., McGlynn, B.L., 2016. The impacts of mountain pine beetle disturbance on the energy balance of snow during the melt period. Hydrol. Process. 30, 588–602.
West, T.O., Marland, G., 2002. A synthesis of carbon sequestration, carbon emissions, and net carbon flux in agriculture: comparing tillage practices in the United States. Agric. Ecosyst. Environ. 91, 217–232.
Wilson, K., Goldstein, A., Falge, E., Aubinet, M., Baldocchi, D., Berbigier, P., Bernhofer, C., Ceulemans, R., Dolman, H., Field, C., Grelle, A., Ibrom, A., Law, B.E., Kowalski, A., Meyers, T., Moncrieff, J., Monson, R., Oechel, W., Tenhunen, J., Valentini, R., Verma, S., 2002. Energy balance closure at FLUXNET sites. Agric. For. Meteorol. 113, 223–243.
Wischmeier, W.H., 1959. A rainfall erosion index for a universal soil-loss equation. Soil Sci. Soc. Am. J. 23, 246–249.
Zhang, Y., Liu, C., Yu, Q., Shen, Y., Kendy, E., Kondoh, A., Tang, C., Sun, H., 2004. Energy fluxes and the Priestley–Taylor parameter over winter wheat and maize in the North China Plain. Hydrol. Process. 18, 2235–2246.